Macromolecular Chemistry and Physics
www.mcp-journal.de

Synergistically Toughening Polyoxymethylene by Methyl Methacrylate–Butadiene–Styrene Copolymer and Thermoplastic Polyurethane

Jing Yang, Wenqing Yang, Xuanlun Wang, Mengyao Dong,* Hu Liu, Evan K. Wujcik, Qian Shao, Shide Wu, Tao Ding,* and Zhanhu Guo**

Ternary polyoxymethylene (POM) blends comprising methacrylate-butadiene-styrene (MBS) copolymer and thermoplastic polyurethanes (TPU) in different weight percentages are prepared by a two-step melt extrusion technique. The synergistic toughening effect of polyoxymethylene by MBS as the impact modifier and TPU as the compatibilizer is investigated. The thermal behaviors of the prepared POM/MBS/TPU blends are analyzed. The notched impact resistance of the modified POM (POM/MBS/TPU 80 wt%/15 wt%/10 wt%) reached 40.83 kJ m^{-2}. The enhanced toughness of the POM/MBS blends with the incorporation of TPU indicates the significance of TPU as a compatibilizer. Although the TPU compatibilizer enhances the interfacial adhesion between POM and MBS and decreases the size of MBS particles, serious agglomeration phenomenon is observed at higher TPU contents (more than 10 wt%) and caused slightly reduced tensile strength and the elongation at break for the sample with both loadings of MBS and TPU at 15 wt%. Instead, further increase of the notched impact strength is noted resulting from the compatibilizer TPU and an effective impact modifier MBS on the POM blend system to achieve a "super-tough" effect. These "super-tough" polyoxymethylene blends can be applied as the host matrix for preparing various multifunctional nanocomposites.

1. Introduction

Nowadays, the composite materials are widely used in different aspects due to thier excellent properties. For example, the nitrogen-doped carbon quantum dots (CQDs) polyvinyl alcohol (PVA) nanocomposites, displaying a long lifetime of 442 ms and an average lifetime of 416 ms at ambient conditions, have potential applications for optical imaging, writing, anti-counterfeiting, or sensors.[1] Modification of materials widens the scope of their applications. For example, the poly(vinylidene

J. Yang, W. Yang, Prof. X. Wang
College of Materials Science and Engineering
Chongqing University of Technology
Chongqing 400054, China
E-mail: wangxuanlun@cqut.edu.cn
Prof. X. Wang
State Key Laboratory of Polymer Materials Engineering
Sichuan University
Chengdu 610065, China
M. Dong, Dr. H. Liu, Prof. Z. Guo
Integrated Composites Laboratory
Department of Chemical & Biomolecular, Engineering
University of Tennessee
Knoxville, TN 37996, USA
E-mail: dmy1989melo@126.com; zguo10@utk.edu
M. Dong, Dr. H. Liu
Key Laboratory of Materials Processing and Mold (Zhengzhou University)
Ministry of Education
National Engineering Research Center for Advanced
Polymer Processing Technology
Zhengzhou University
Zhengzhou 450002, China
The ORCID identification number(s) for the author(s) of this article can be found under https://doi.org/10.1002/macp.201800567.
Prof. E. K. Wujcik
Materials Engineering and Nanosensor [MEAN] Laboratory
Department of Chemical and Biological Engineering
The University of Alabama
Tuscaloosa, AL 35487, USA
Prof. Q. Shao
College of Chemical and Environmental Engineering
Shandong University of Science and Technology
Qingdao 266590, China
Prof. S. Wu
Henan Provincial Key Laboratory of Surface and Interface Science
Zhengzhou University of Light Industry
Zhengzhou 450001, China
Prof. T. Ding
College of Chemistry and Chemical Engineering
Henan University
Kaifeng 475004, China
E-mail: dingtao@henu.edu.cn

DOI: 10.1002/macp.201800567

fluoride) (PVDF) ultrafiltration (UF) membrane modified by catechol-functionalized poly(ethylene glycol) (Cate-PEG) exhibited a high water flux, good bovine serum albumin (BSA) rejection, and a satisfactory antifouling performance after the BSA solution cycling tests.[2a] PVDF porous membranes integrated with mussel-inspired coating and in situ silicification via "pyrogallol-amino covalent bridge" demonstrated excellent antifouling performance and great water treatments toward environmental remediation.[2b] Biopolymer 2S-soy protein (extracted from soy protein isolate (2S-SPI)) functionalzied carbon nanofiber (CNFs) demonstrated a better disperion of CNFs in PVDF. The formed nanocomposites with functionalized CNFs demonstrated a dominant long-range charge hopping electrical conduction, different from the Maxwell–Wagner–Sillars (MWS) relaxation dominat electrical condution observed in the nanocomposites with untreated CNFs.[3] 2S-SPI modification also led to a strong coupling between conductivity relaxation and MWS relaxation in the PVDF nanocomposites, accompanied by greater enhancement of conductivity relaxation.[3] Meanwhile, compared with pure carbon, metal, or ceramics,[4] flexible engineering plastics can make machine parts at much lower temperatures and easier processing methods. Especially, with high mechanical strength and rigidity, creep resistance, good chemical resistance, and remarkable wear resistance, plastics based nanocomposites have been applied in various fields such as electronics industry, automobiles, aerospace industry, electromagnetic interface (EMI) shielding, sensors, and so on.[5–11] Polyoxymethylene (POM) has a simple backbone without side groups attached, and thus has a fast crystallization process that leads to poor impact strength and prone to cracking. Modification of the POM is necessary. Different techniques for toughening POM have been reported. Two main methods have been demonstrated to improve the fracture toughness of POM including the usage of elastomers or rigid particles as a toughener.

Applying low modulus elastomers as a toughener is a useful method for modifying POM. It has been confirmed from earlier experimental and theoretical results that its notched impact resistance can be effectively improved by adding thermoplastic polyurethane (TPU).[11–15] TPU not only can transfer the load effectively but also impart good interfacial interaction to POM, thus significantly increases the fracture toughness of POM. For example, Pielichowshi et al.[11] observed the decrease in melting enthalpy of POM/TPU blend with increasing the amount TPU up to 10 wt%, without affecting the crystalline nature of POM. TPU was distributed uniformly in POM due to the presence of specific hydrogen bond interaction between the oxygen in the ether of POM and hydrogen in the urethane of TPU. Although the increase in TPU content contributed to a greater elongation at break, POM/TPU blends did not show "super-tough" behavior at room temperature.[16] In addition, TPU is expensive. Therefore, other less expensive toughenens are sought to modify POM.

Graft copolymers having a core-shell structure (such as methacrylate-butadiene-styrene copolymer [MBS] or acrylonitrile butadiene styrene [ABS]) have been tested as the elastomer component.[17,18] Typical impact modifiers include not only aromatic polyurethanes but also acrylic-type polymers like MBS copolymer. MBS as a core-shell impact modifier (polymerized styrene-butadiene rubber as the core and polymethyl methacrylate as the shell) is cheaper than TPU, and it has good processing performance. MBS is useful as an impact modifier in engineering plastics. For the used core-shell impact modifiers, MBS typically has good anti-blocking properties and is easy to process.[19]

Despite widespread availability, the poor compatibility of POM with other polymers limits its applications.[5] For instance, reduced interfacial adhesion was observed between POM and most toughening agents.[9,19–24] Kumar et al. demonstrated that the addition of poly(acrylic acid)-grafted polypropylene (PGP) into POM/ethylene-proplene-diene monomer (EPDM) blend as compatibilizer improved its impact strength.[20] The unsatisfactory mechanical performance arising from high interfacial tension between the polymers is ameliorated by the incorporation of PGP. Yang et al. found that the POM /ethylene-butyl acrylate copolymer (EBA) blend compatibilized with ethylene-methyl acrylate-flycidyl methacrylate copolymer (EMA-GMA) exhibited a higher impact strength than that without compatibilizer.[21] Thus, the compatibility between POM and toughener is deemed to be the key factor to determine the toughening effect of POM. Wang et al. demonstrated that adding ionomers also improved the interfacial properties between MBS and POM, which in turn improved the stress transfer between POM and MBS.[19] The ionomer acted as both compatibilizer and impact modifier, thereby improving the compatibility and mechanical performance of the POM/MBS blend. However, using both compatibilizer and impact modifier simultaneously toughening polyoxymethylene has not been reported yet.

In this work, the toughness of POM blends was improved by using combined MBS modifier and the reactive TPU compatibilizer. The toughening effects of TPU to POM/MBS blends with different weight percentages were studied. The mechanical properties, crystallization, rheological behavior, and morphology of the prepared ternary POM blends were investigated in detail as well.

2. Experimental Section

2.1. Materials

Polyoxymethylene (M90) was procured from Yunnan Yuntianhua Co., Ltd., China. The impact modifier methyl methacrylate-butadiene-styrene (MBS) copolymer (EM500) was obtained from LG, Korea. The compatibilizer TPU (1075A) and the antioxidant (K1010) were bought from BASF, China. Calcium hydroxide (JYH-S01) was procured from Hongyu Calcium Co Ltd., China. All the chemicals were commercial grade.

2.2. Preparation of Toughened POM Blends

POM and TPU were dried before the extrusion process in an electric blast drying oven (Model:BPG-9070A, Blue Pard, China) at 80 °C for 3 h to eliminate the residual moisture. The ternary blends comprising their constituents at different weight

Table 1. Experimental formulation of POM/MBS/TPU blends.

Sample code	POM [wt%]	MBS [wt%]	TPU [wt%]
T-0	80	15	0
T-5	80	15	5
T-10	80	15	10
T-15	80	15	15

ratios were prepared in two consecutive steps using the co-rotating twin-screw extruder (Model: TSE-30A,L/D = 40:1, Nanjing Ruiya Polymer Processing Equipment Co Ltd., China). In the first step, the toughening masterbatches were prepared by using MBS and TPU in various ratios, with the addition of the antioxidant (0.5 wt% for the total mass of MBS and TPU) and calcium hydroxide (1 wt% for the total mass of MBS and TPU). The purpose of using calcium hydroxide is to make toughening masterbatches neutral since MBS is acid and can make polyoxymethylene decompose much easier. The neutral toughening masterbatches will not have a problem of easy decomposition of polyoxymethylene. The extrusion temperatures along the barrel were set between 110 and 185 °C. The screw was maintained at 200 rpm. Then, the residual moistures were removed from the toughening masterbatches by drying at 40 °C for 12 h to ensure the removal of moisture before the extrusion process. In the second step, these masterbatches were blended with POM at different weight ratios. The extrusion temperatures along the barrel were the same as those in the first step. The dumbbell and rectangular shaped specimens to analyze the mechanical properties were obtained using injection molding machine (Model: EM80-SVP/2, Zhen Xiong Company, Taiwan). The POM blend granules were dried prior to the injection molding process. The compositions of prepared ternary blends are summarized for clarity in **Table 1**.

2.3. Characterizations

2.3.1. Mechanical Property Measurements

The tensile properties were measured using dumbbell-shaped test specimens at 20 mm min^{-1} using an electronic universal testing machine (Model: CMT 6104, MTS systems, China) according to GB/T 1040. 2–2006. The notched Izod impact resistance (Izod) was evaluated using a pendulum impact tester (Model: ZBC1400-b, Pendulum bob = 2.75 J, MTS systems, China) according to GB/T 1843–2008. In both impact test and tensile test, at least five samples were tested for each species. All the impact tests and tensile tests were carried out at 25 °C. The mechanical results were calculated as a function of the original cross section.

2.3.2. Thermal Analysis

Differential scanning calorimetry (DSC) thermograms were recorded (Model:DSC-Q20, TA Instruments, USA) in the temperature range between 40 and 200 °C to examine the crystallization behavior of the prepared ternary blends. The samples of ≈3–5 mg were heated at 10 °C min^{-1} under N_2 atmosphere (50 mL min^{-1}) and subsequently cooled down at 10 °C min^{-1} to get the crystallization curves. The degradation behavior was examined between 25 and 600 °C using thermogravimetric analyzer (TGA, Model:TGA-Q50, TA Instruments Co Ltd., USA) by heating the samples at 10 °C min^{-1} in N_2 atmosphere (60 mL min^{-1}).

2.3.3. Dynamic Rheological Behavior

Rheological behavior of the prepared blends was studied using an AR-1500ex rotational rheometer (TA Instruments Co Ltd., USA) with a steel plate of 25 mm in diameter. An isothermal dynamic frequency sweep between 0.01 and 100 Hz was performed at the strain amplitude, temperature, and testing gap of 3%, 185 °C, and 1 mm, respectively.

2.3.4. Dynamic Mechanical Analysis

The dynamic characteristics of the injection molded samples (35 mm × 10 mm × 4 mm) were analyzed under Multi-Frequency-Strain testing mode (Model: DMA Q800, TA Instruments Co Ltd., USA), between 35 and 160 °C at 3 °C min^{-1} with a single frequency of 10 Hz.

2.3.5. Morphological Studies

The microstructures of the impact fractured specimen surfaces were observed using a scanning electron microscope (Model: JSM-6460LV, JEOL, Japan).

3. Results and Discussion

3.1. Mechanical Performance

The mechanical properties of pristine POM, POM/MBS blends with and without TPU are summarized in **Table 2**. According to Table 2, the elongation at break (ε_B) of the modified POM at 15 wt% MBS content reached 108.67%, which was 76.18% more than that of pristine POM (61.68%). Hence, it improved the toughness of POM blends drastically. Meanwhile, TPU as a

Table 2. Mechanical properties of samples.

Code	σ_M [a]	Std.	ε_B [b]	Std.	*Izod* [c]	Std.
POM	60. 34	0.205	61. 68	5.42	16. 36	1.31
T-0	44. 63	0.43	108. 67	4.36	28. 25	0.52
T-5	39. 85	0.35	193. 35	6.21	37. 19	1.60
T-10	38. 90	0.15	222. 51	6.45	40. 83	1.13
T-15	35. 79	0.26	186. 05	8.08	44. 93	2.09

[a]Tensile strength (MPa); [b]Elongation at break (%); [c]Notched Izod impact strength (kJ m^{-2}).

compatibilizer was added to the blends, and the amount of TPU in the blends steadily increased. At 10 wt% of TPU, the percentage of breaking elongation (ε_B) of the ternary blends (T-10) reached a peak of 222.51%, which was 260.75% higher than that of pristine POM (61.68%). At 15 wt%, the ε_B dropped down to 186.05%, but still larger than that of pristine POM. This phenomenon resulted from severe agglomeration (Figure 5e), which hinders the dispersion effect of MBS in the POM matrix in a relatively high content of TPU (e.g., 15 wt% by weight).

MBS is an excellent core-shell toughener for modifying POM. The elongation at break of the modified POM was increased quickly when only MBS and POM were blended. The elongation at break of 28.25 kJ m^{-2} was reached, and this illustrated that MBS could indeed toughen polyoxymethylene effectively. Similar phenomenon has been obsereved in other systems. For example, the toughness mechanism of MBS/polylactic acid (PLA) blends is observed to include the shear yielding of the PLA matrix and the cavitation of MBS particles.[25] In this investigation, TPU as compatibilizer was added to modify POM to ameliorate the poor compatibility of MBS dispersion phase particles with the POM matrix. Hydrogen bonding which was formed between POM and TPU could improve the interfacial interaction between them. Both POM and MBS had an ester structure, strong polarity, and good compatibility with TPU.[11] The Izod impact strength of T-5 (15 wt% TPU content) reached 37.19 kJ m^{-2} and had been greatly improved. At 15 wt%, the Izod impact strength of POM/MBS/TPU blends reached 44.93 kJ m^{-2}, which was 174.63% higher than the Izod impact strength of pristine POM (16.36 kJ m^{-2}) to achieve a "supertough" effect. Despite the decrease in elongation at break due to agglomeration, the Izod impact strength was still improved which was attributed to the added TPU acting as an excellent and effective toughener for polyoxymethylene.

On the other hand, according to Table 2, POM/MBS blends exhibited a lower tensile strength than the pristine POM. The tensile strength was gradually decreased for POM/MBS/TPU blends with a gradually decreased mass ratio of POM after adding MBS and TPU. The reduced tensile strength was due to the weak tensile strength of both MBS and TPU in comparison to the pristine POM. When the percentages of MBS and TPU were both at 15 wt%, the tensile strength of the blends (sample code: T-15) was 35.79 MPa, lower than that of pure POM (60.34 MPa) by 42.79%, but still above 30 MPa. It illustrates that the tensile strength was well maintained while the toughness of the blends was increased gradually.

3.2. Thermal Analysis

Figure 1 depicts the crystallization behavior of pristine POM and ternary POM/MBS/TPU blends. The thermal parameters, including enthalpy, crystallinity, initial crystallization temperature, and crystallization peak temperature are listed in **Table 3**. It was found that ΔH was decreased continuously with the reduction of the POM content. The crystallinities of POM in the blends were calculated using Equation (1).[26]

$$\text{Crystallinity } (X_c) = \frac{\Delta H_m^{\text{sample}}}{\Delta H_m^0} \times 100\% \quad (1)$$

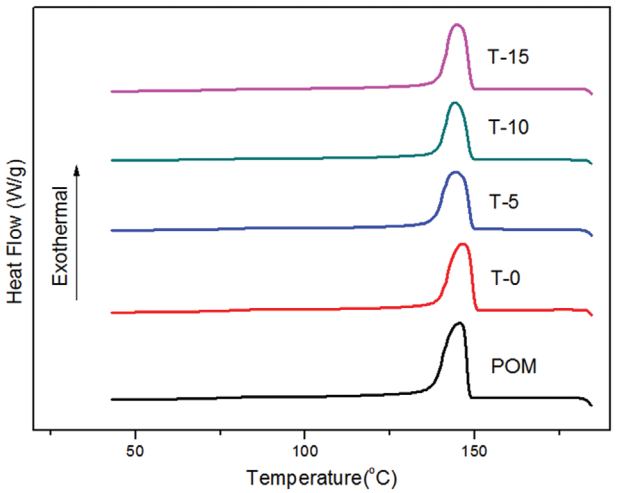

Figure 1. DSC cooling thermogram of various POM/MBS/TPU blends.

where $\Delta H_m^{\text{sample}}$ is the enthalpy of fusion of the blends, ΔH_m^0 is the theoretic value of enthalpy at X_c = 100% (190 J g^{-1}).[23]

The POM blends toughened by MBS exhibited a lower crystallinity than the pristine POM. The crystallinity of T-0 (0 wt% TPU content) was 75.15%, slightly lower than that of pristine POM (75.68%). The dispersed MBS phase existed as small particles, which were uniformly distributed in the POM matrix with a large interfacial area as verified by the SEM images (Figure 5). The adhesion of amorphous state POM chain segments at the interface resulted in a decrease of crystallinity. Otherwise, the crystallinity of POM/MBS blends with TPU was lower than that of POM/MBS blends without TPU (T-0). This was because the interfacial interactions and dispersion between POM and MBS were enhanced in the presence of the compatibilizer TPU. The X_c was found to be minimum (74.12%) when the TPU content was 10 wt%. The compatibilizer effect of TPU in the POM/MBS blends was decreased with increasing the TPU content (above 10%) because of its aggregation. Hence, the X_c of T-15 was increased slightly. The thermal parameters presented in Table 3 implied that the addition of MBS and TPU did not change the crystallization of POM. For instance, the initial crystallization temperature (T_{co}) and the peak crystallization temperature (T_{cm}) of the blends were about 148 and 145 °C, respectively.

Figure 2 shows the TGA curves of pristine POM, TPU, MBS, and POM/MBS blends with and without TPU. The onset degradation temperature (T_{onset}) (the temperature at 5 wt% weight loss) of the POM, TPU, MBS, and POM/MBS blends are presented in **Table 4**. It can be observed that the

Table 3. Crystallization parameters for various POM/MBS/TPU blends.

Sample code	ΔH [J g^{-1}]	XC [%]	T_{co} [°C]	T_{cm} [°C]
POM	143. 80	75. 68	148. 24	145. 69
T-0	120. 24	75. 15	148. 85	145. 59
T-5	113. 01	74. 35	148. 13	145. 45
T-10	107. 30	74. 12	148. 84	145. 28
T-15	103. 20	74. 68	148. 01	145. 88

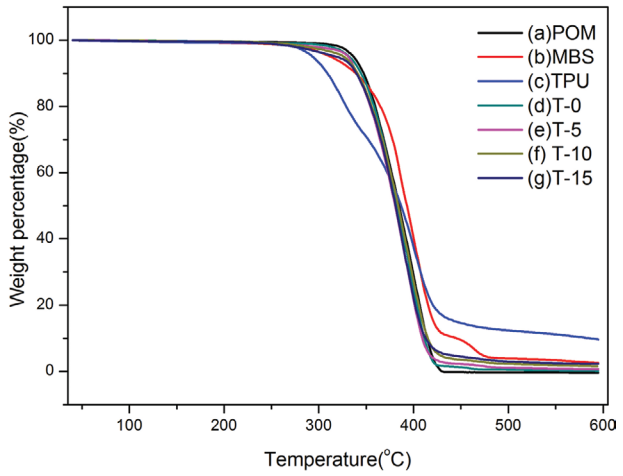

Figure 2. The TGA thermograms of POM, MBS, TPU, and various POM/MBS/TPU blends.

Table 4. Onset degradation temperatures of the samples.

Sample code	POM	MBS	TPU	T-0	T-5	T-10	T-15
T_d [°C]	335. 24	312. 03	294. 58	332. 62	331. 81	326. 36	318. 42

T_{onset} of POM (335.24 °C) was higher than other samples while TPU (294.58 °C) showed the lowest. The T_{onset} of 312.03 °C for MBS is 23.21 °C lower than that for the POM. Therefore, the T_{onset} of the prepared blends decreased with the inclusion of MBS. Their T_{onset} further decreased with the addition of TPU. When only MBS was added to the POM blends, the T_{onset} of T-0 was 332.62 °C. When both the MBS and TPU were added to the POM, the T_{onset} was reduced to 331.81 °C for T-5. Moreover, the T_{onset} of the polymer blends was further decreased with the increase of TPU in the blends. It is likely that MBS and TPU initiated their degradation, and eight of the blends began to decrease, and the T_{onset} of the integral blends was also decreased. Thus, the thermal stability of the polymer blends was further weakened with the increase of TPU in the blends.[27,28]

3.3. Dynamic Mechanical Analysis

Dynamic storage modulus (E′) and dynamic loss modulus (E″) of pristine POM, MBS, and POM/MBS blends as a function of temperature are depicted in **Figure 3**a,b, respectively. The E′ and E″ of pristine POM were observed to be much higher than those of pristine MBS, except that the variation of E′ and E″ of MBS with respect to the temperature occurred as a thread

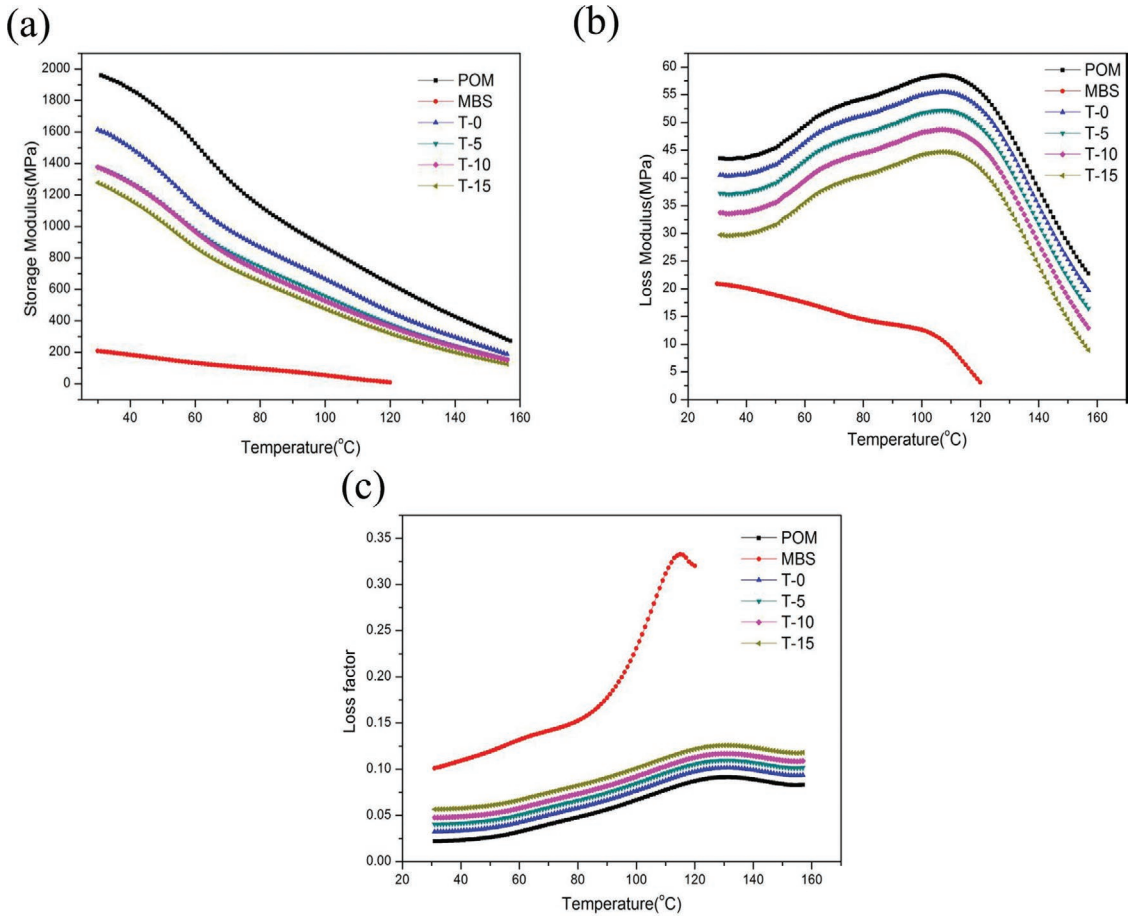

Figure 3. a) Storage modulus; b) loss modulus; and c) loss factor versus temperature curve of various POM/MBS/TPU blends.

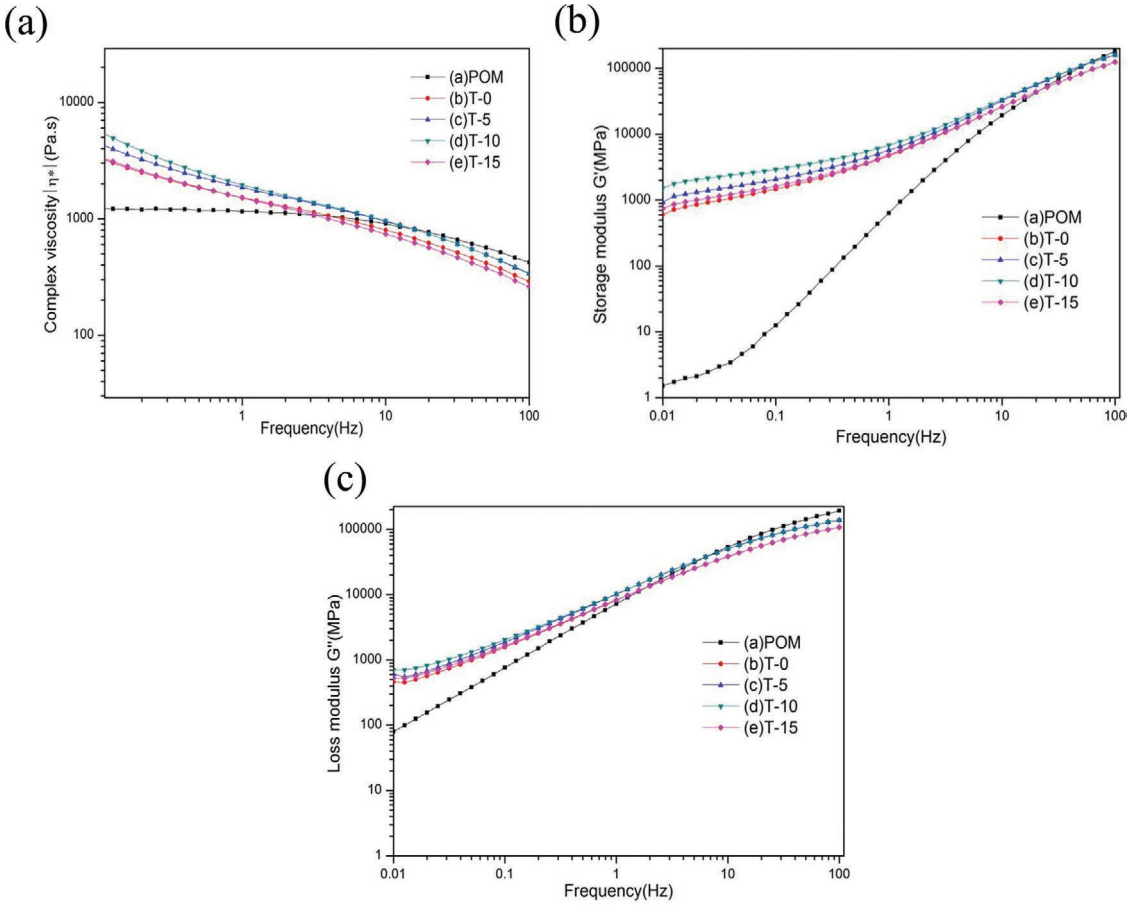

Figure 4. Time-temperature superposition of a) complex viscosity; b) G′; and c) G″ of POM, POM/MBS blends and POM/MBS/TPU blends.

breakage after 120 °C due to its low melting point. Hence, the E′ and E″ of POM/MBS blends (T-0) began to decrease with the addition of MBS. Furthermore, the E′ and E″ of POM/MBS/TPU blends decreased with the addition of TPU since it is a soft thermoplastic elastomer having a low E′ and E″. The E′ was generally related to the "stiffness" of a polymer.

Figure 3a shows that the dynamic modulus decreased with increasing the TPU content for POM/MBS/TPU blends. But the dynamic modulus of POM/MBS/TPU blends (Figure 3a-T-15 and Figure 3b-T-15) was much higher than that of MBS (Figure 3a-MBS and **Figure 4**b-MBS). It could be explained that the E′ and E″ of POM/MBS/TPU blends, which had a "sea-island" structure, depend on the E′ and E″ of the POM matrix.[29,30]

The dependence of tan δ as a function of temperature for pristine POM, MBS, POM/MBS blends with and without TPU is depicted in Figure 3b. Obviously, the tanδ for MBS was much higher than that of POM, except that the tanδ for pure MBS suddenly became zero when the temperature reached above 120 °C due to the low melting point of MBS. It is also observed that the tanδ values of the polymer blends are higher than this of pristine POM. Further, its tanδ increased with the increase in the TPU content due to a higher loss factor of TPU as an elastomer. When the content of TPU was 15 wt%, the tanδ of T-15 was the largest compared with all the toughened POM blends. Before the α relaxation (i.e., the melting) of POM, the tanδ increased with the temperature. This phenomenon could be due to the increase in the loss factor of the blend while its E′ was decreased. The α relaxation resulted from the removal of chain segments from the POM crystals at a higher temperature. In this study, the tanδ peak for the toughened POM blends was about 0.075–0.115. A larger loss factor indicates more heat loss.

3.4. Rheological Properties

Figure 4 shows the complex viscosity ($|\eta^*|$), storage modulus (G') and loss modulus (G'')—frequency of pristine POM and its blends, which were obtained by shifting the frequency to a reference temperature of 185 °C. The $|\eta^*|$ of all the samples decreased significantly as a function of frequency (see Figure 4a), which was attributed to their strong shear thinning behavior. Apparently, in the lower frequency region, the $|\eta^*|$ of the POM blends was higher than this of the pristine POM. Further, the $|\eta^*|$ of the POM blends increased with the addition of TPU (Figure 4c,d). This can be ascribed to the enhanced interfacial adhesion caused by the strong bonding of TPU molecular chains at the POM/MBS interface.[31] Subsequently,

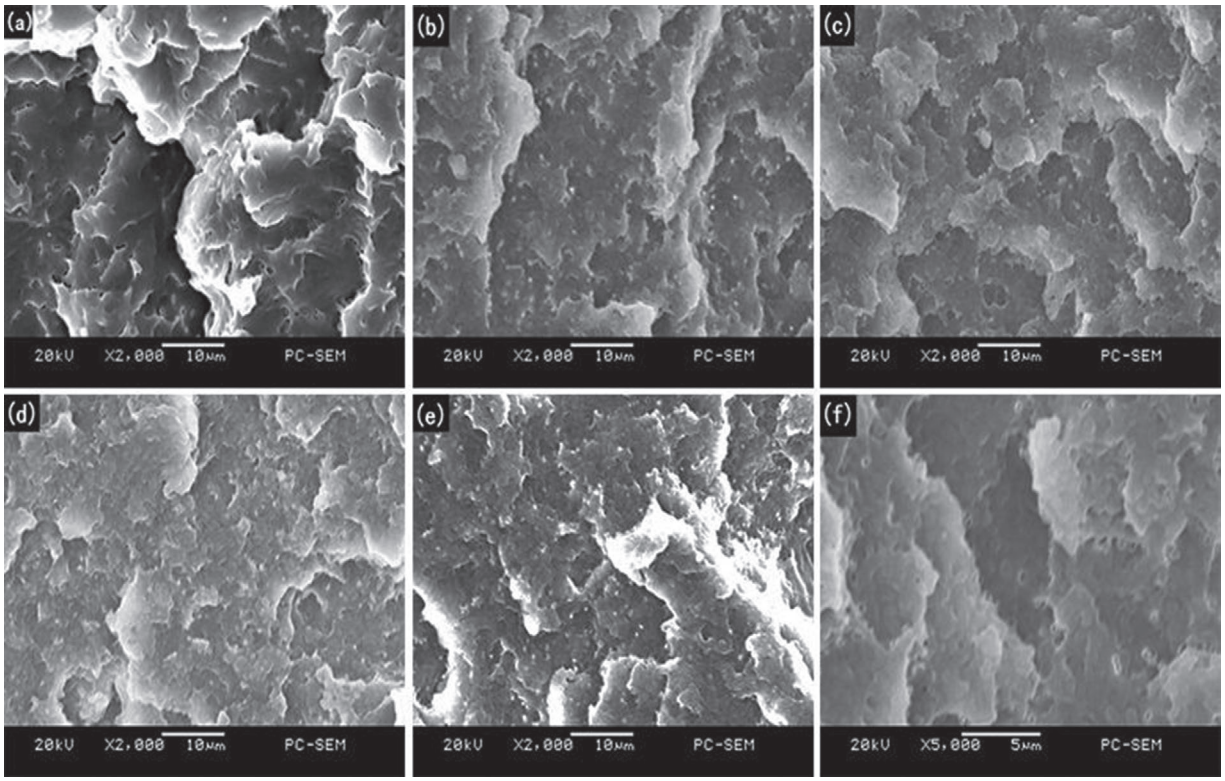

Figure 5. SEM microscopic photos of impact-fractured surfaces of various POM/MBS/TPU blends: a) POM; b) T-0; c) T-5; d)T-10; e) T-15; and f) T-0* (the impact-fractured surfaces of T-0 was magnified 5000 times).

this enhanced interfacial adhesion at the interface between the POM and MBS contributed to a better stress transfer. However, it is important to note that a jump in the complex viscosity occurred when the content of TPU was 15 wt%. This was because of more pronounced agglomeration with adding more TPU. Meanwhile, in the higher frequency region, the $|\eta^*|$ of the toughened POM blends was lower than this of POM. This phenomenon demonstrates that the shear thinning behavior of MBS was stronger compared to that of POM.

Figure 4b,c shows the variation of storage modulus(G′) and loss modulus(G″) of POM and its binary and ternary blends, respectively. For one thing, in the lower frequency region, both G′ and G″ increased linearly when increasing the frequency over the whole compositions. This is attributed to the longer relaxation time that is enough for the polymer chains to release the entanglement at the lower frequencies. In the higher frequency region, there was not enough time for relaxation, thus resulted in both higher G′ and G″.[32] In addition, the G′ and G″ of POM/MBS blends were much higher than those of POM in the low-frequency zone. A linear increase of the G′, as well as G″ of POM/MBS/TPU blends, was observed when the content of TPU varied from 0 wt% to 10 wt%. Especially, the G′ and G″ of POM/MBS/TPU blends at 10 wt% reached the maximum. However, it should be noted that the G′ and G″ of POM/MBS/TPU blends (Figure 4b-T-15 and Figure 4c-T-15) were also higher than those of POM/MBS blends (Figure 4b-T-0 and Figure 4c-T-0), but lower than those of the blends containing 5 wt% and 10 wt% of TPU. The incorporation of TPU as a compatibilizer into POM/MBS blends resulted in an enhanced interfacial adhesion between the POM matrix and MBS particles. Moreover, a less efficient compatibilization resulted from serious agglomeration due to the relatively high content of TPU at 15 wt%. In conclusion, storage modulus (G') and loss modulus (G'') of T-5, T-10, and T-15 were also higher than those of POM/MBS blends without TPU (T-0), indicating that TPU was a good compatibilizer for the POM/MBS blends.

3.5. Morphology of Fractured Surfaces

Figure 5 shows the SEM impact fracture surfaces of the POM blends. The observed smooth surface (Figure 5a) demonstrated that POM is a brittle material. Dispersed phase MBS particles were found in the POM matrix (Figure 5b) when POM was blended with MBS. The addition of MBS caused the blends to become coarser (Figure 5f) than the virgin POM. This implies that the toughness of the blends had been improved. The trend clearly shows that the impact-fractured surfaces of POM/MBS became much coarser (Figure 5c,d) after compatibilization with TPU, resulting in a higher toughness of the ternary blends. This phenomenon was demonstrated through mechanical property tests. The smaller the MBS particles were, the more uniform the particle distribution was. So, this created a better toughening effect. In the absence of TPU (compatibilizer), the particle size in the dispersed phase strongly depended on its contents. A higher amount of dispersed phase corresponded to

a more serious agglomeration. Furthermore, the particle size distribution was widened with respect to the dispersed phase. The compatibilizer could not reduce the tension at the interface but stabilized the interface to hamper the agglomeration.[33] Hence, the notched impact strength (37.19 kJ m^{-2}) of POM/MBS/TPU blends was a little higher than that (28.25 kJ m^{-2}) of POM/MBS blends without TPU as a compatibilizer. This confirms that it is necessary to add TPU as a compatibilizer. The particle size and elastomeric property of an impact modifier along with its interfacial adhesion determine the toughening effect.[25] At 15 wt% of TPU, the large particle size of the MBS phase and a wide particle size distribution were observed (Figure 5e). This phenomenon was the result of serious agglomeration with a less effective compatibilization. Notably, the notched impact strength (44.93 kJ m^{-2}) of T-15 was higher than that of T-10 (40.83kJ m^{-2}), indicating that TPU was a better toughening agent for POM. The SEM image (Figure 5f) shows that there were many fine fibrous substances at the edge of the fracture surface. This indicates that the MBS particles absorbed energy as they were drawn into fibers. Therefore, the toughness of the material was greatly improved.

4. Conclusions

Mechanically improved POM blends comprising MBS and TPU as the impact modifier and the compatibilizer, respectively, were prepared by a two-step melt extrusion technique. For one thing, the prepared ternary blends exhibited the "super-tough" effect. At 15 wt% of TPU, the elongation at break, and tensile strength of POM blend (T-15) decreased due to the agglomeration caused by the relatively high content of TPU. However, the notched impact strength of T-15 reached 44.93 kJ m^{-2}. The morphological analysis depicted that the impact fractured surface of pristine POM was smooth, while the impact fractured surface of POM/MBS/TPU blends became rougher and contained tiny fibrous materials. It indicated that the shape of MBS in the dispersed phase was stretched to become fibrous and enabled to absorb a lot of energy so that the toughness of blends was improved. SEM images indicated that the MBS particles became smaller and were distributed more uniformly with the addition of TPU to create a better toughening effect. This confirmed that the addition of a TPU compatibilizer was very necessary. For these reasons, the incorporation of TPU (lower than 15 wt%) into POM/MBS blends resulted in a decrease in crystallinity within the crystallization temperature range. This also resulted in an increase in $|\eta^*|$, G′, and G″ of the blends in a low-frequency region. Although the addition of the TPU compatibilizer resulted in an enhanced interfacial adhesion between POM and MBS particles, there was serious agglomeration with higher TPU contents (more than 10 wt%). For these reasons, when the content of TPU reached 15 wt%, it resulted in a slight increase in the crystallinity of the blends and the $|\eta^*|$, and G′ and G″ of the blends were on the decrease. On the other hand, the TGA thermograms showed that the thermal stability of the blends was further weakened with the increase of TPU and MBS in the blends. Dynamic storage modulus (E′) and dynamic loss modulus (E″) of the blends are lower than those of pristine POM. In conclusion, the optimal weight ratio for the POM/MBS/TPU blends was found to be 80:15:10. This study provided a facile approach to develop low cost "super-tough" polyoxymethylene composites, thereby empowering the commercial utilization of polymer composites with improved mechanical properties. These "super-tough" polyoxymethylene blends can be applied as the host matrix for nanocomposites.[34,35] This method not only reduces the cost but also makes the POM blends more attractive to industries for different applications like EMI shielding,[36] strain sensing.[37]

Acknowledgements

This study was financially supported by the Opening Project of State Key Laboratory of Polymer Materials Engineering (Sichuan University) (Grant No. sklpme2018-4-26).

Conflict of Interest

The authors declare no conflict of interest.

Keywords

compatibilization, methacrylate-butadiene-styrene, polyoxymethylene, super-tough effect, thermoplastic polyurethanes

Received: December 21, 2018
Revised: April 9, 2019
Published online: May 9, 2019

[1] X. Wu, W. Li, P. Wu, C. Ma, Y. Liu, M. Xu, S. Liu, *Eng. Sci.* **2018**, *4*, 111.
[2] a) H. Sun, X. Yang, Y. Zhang, X. Cheng, Y. Xu, Y-P. Bai, L. Shao, *J. Membr. Sci.* **2018**, *563*, 22; b) X. Yang, H. Sun, A. Pal, Y. Bai, L. Shao, *ACS Appl. Mater. Interfaces* **2018**, *10*, 29982.
[3] Z. Zheng, O. Olayinka, B. Li, *Eng. Sci.* **2018**, *4*, 87.
[4] a) W. Xie, X. Zhu, S. Yi, J. Kuang, H. Cheng, W. Tang, Y. Deng. *Mater. Des.* **2016**, *90*, 38; b) K. Le, Z. Wang, F. Wang, Q. Wang, Q. Shao, V. Murugadoss, S. Wu, W. Liu, J. Liu, Q. Gao, Z. Guo, *Dalton Trans.* **2019**, *48*, 5193; c) W. Xie, H. Cheng, Z. Chu, Z. Chen, C. Long, *Ceram. Int.* **2011**, *37*, 1947; d) Y. Zhao, F. Liu, J. Tan, P. Li, Z. Wang, K. Zhu, X. Mai, H. Liu, X. Wang, Y. Ma, Z. Guo, *J. Alloys Compd.* **2019**, *772*, 186; e) Z. Lin, B. Lin, Z. Wang, S. Chen, C. Wang, M. Dong, Q. Gao, Q. Shao, S. Wu, T. Ding, H. Liu, Z. Guo, *ChemCatChem* **2019**, *11*, 2217; f) Z. Zhao, P. Bai, L. Li, J. Li, L. Wu, P. Huo, L. Tan, *Materials* **2019**, *12*, 330; g) Z. Zhao, J. Li, P. Bai, H. Qu, M. Liang, H. Liao, L. Wu, P. Huo, H. Liu, J. Zhang, *Metals* **2019**, *9*, 267; h) Y. Zhao, B. Zhang, H. Hou, W. Chen, M. Wang, *J. Mater. Sci. Technol.* **2019**, *35*, 1044; i) Y. Zhao, L Qi, Y Jin, K. Wang, J. Tian, P. Han, *J. Alloys Compd.* **2015**, *647*, 1104; j) Y. Zhao, X. Tian, B. Zhao, Y. Sun, H. Guo, M. Dong, H. Liu, X. Wang, Z. Guo, A. Umar, H. Hou, *Sci. Adv. Mater.* **2018**, *10*, 1793; k) C. Hou, Z. Tai, L. Zhao, Y. Zhai, Y. Hou, Y. Fan, F. Dang, J. Wang, H. Liu, *J. Mater. Chem. A* **2018**, *6*, 9723; l) Z. Zhao, P. Bai, R. Misra, M. Dong, R. Guan, Y. Li, J. Zhang, L. Tan, J. Gao, T. Ding, W. Du, Z. Guo, *J. Alloys Compd.* **2019**, *792*, 203.
[5] a) S. Singh, C. Ching, C. Abdullah, Y. Ching, S. Razali, N. Gan, *Polymers* **2018**, *10*, 338; b) H. Sun, Z. Yang, Y. Pu, W. Dou, C. Wang, W. Wang, X. Hao, S. Chen, Q. Shao, M. Dong, S. Wu, T. Ding,

Z. Guo, *J. Colloid Interface Sci.* **2019**, *547*, 40; c) F. Niu, R. He, J. Li, *Surf. Interface Anal.* **2018**, *50*, 96; d) S. Bai, Q. Wang, *J. Vinyl Addit. Technol.* **2016**, *22*, 479; e) A. Das, S. Suin, N. Shrivastava, S. Maiti, J. Mishra, B. Khatua, *Polym. Compos.* **2014**, *35*, 273; f) L. Guo, X. Xu, Y. Zhang, Z. Zhang, *Polym. Compos.* **2014**, *35*, 127; g) R. Ma, Y. Wang, H. Qi, C. Shi, G. Wei, L. Xiao, Z. Huang, S. Liu, H. Yu, C. Teng, H. Liu, V. Murugadoss, J. Zhang, Y. Wang, Z. Guo, *Composites, Part B* **2019**, *167*, 396; h) S. Shi, L. Wang, Y. Pan, C. Liu, X. Liu, Y. Li, J. Zhang, G. Zheng, Z. Guo, *Composites, Part B* **2019**, *167*, 362.

[6] a) C. Wang, B. Mo, Z. He, Q. Shao, D. Pan, E. Wujick, J. Guo, X. Xie, X. Xie, Z. Guo, *J. Membr. Sci.* **2018**, *556*, 118; b) C. Wang, B. Mo, Z. He, C. X. Zhao, L. Zhang, Q. Shao, X. Guo, E. Wujcik, Z. Guo, *Polymer* **2018**, *138*, 363; c) S. Sun, L. Zhu, X. Liu, L. Wu, K. Dai, C. Liu, C. Shen, X. Guo, G. Zheng, Z. Guo, *ACS Sustainable Chem. Eng.* **2018**, *6*, 9866; d) Y. Qian, Y. Yuan, H. Wang, H. Liu, J. Zhang, S. Shi, Z. Guo, N. Wang, *J. Mater. Chem. A* **2018**, *6*, 24676; e) G. Zhu, X. Cui, Y. Zhang, M. Dong, H. Liu, Q. Shao, T. Ding, S. Wu, Z. Guo, *Polymer* **2019**, *172*, 415.

[7] a) X. Gong, Y. Liu, Y. Wang, Z. Xie, Q. Dong, M. Dong, H. Liu, Q. Shao, N. Lu, V. Murugadoss, T. Ding, Z. Guo, *Polymer* **2019**, *168*, 131; b) J. Guo, H. Song, H. Liu, C. Luo, Y. Ren, T. Ding, M. Khan, D. Young, X. Liu, X. Zhang, J. Kong, Z. Guo, *J. Mater. Chem. C* **2017**, *5*, 5334; c) Z. Hu, Y. Liu, X. Xu, W. Yuan, L. Yang, Q. Shao, Z. Guo, T. Ding, Y. Huang, *Polymer* **2019**, *164*, 79; d) Z. Hu, D. Zhang, F. Lu, W. Yuan, X. Xu, Q. Zhang, H. Liu, Q. Shao, Z. Guo, Y. Huang, *Macromolecules* **2018**, *51*, 5294; e) Y. He, Q. Chen, S. Yang, C. Lu, M. Feng, Y. Jiang, G. Cao, J. Zhang, C. Liu, *Composites, Part A* **2018**, *108*, 12; f) H. Gu, X. Xu, M. Dong, P. Xie, Q. Shao, R. Fan, C. Liu, S. Wu, R. Wei, Z. Guo, *Carbon* **2019**, *147*, 550; g) D. Jiang, V. Murugadoss, Y. Wang, J. Lin, T. Ding, Z. Wang, Q. Shao, C. Wang, H. Liu, N. Lu, R. Wei, S. Angaiah, Z. Guo, *Polym. Rev.* **2019**. https://doi.org/10.1080/15583724.2018.1546737; h) L. Chen, J. Zhao, L. Wang, F. Peng, H. Liu, J. Zhang, J. Gu, Z. Guo, *Ceramics Inter.* **2019**, *45*, 11756; i) N. Wu, C. Liu, D. Xu, J. Liu, W. Liu, H. Liu, J. Zhang, W. Xie, Z. Guo, *J. Mater. Chem. C* **2019**, *7*, 1659; j) N. Wu, D. Xu, Z. Wang, F. Wang, J. Liu, W. Liu, Q. Shao, H. Liu, Q. Gao, Z. Guo, *Carbon* **2019**, *145*, 433; k) C. Wang, V. Murugadoss, J. Kong, Z. He, X. Mai, Q. Shao, Y. Chen, L. Guo, C. Liu, S. Angaiah, Z. Guo, *Carbon* **2018**, *140*, 696.

[8] a) Z. Wu, S. Gao, L. Chen, D. Jiang, Q. Shao, B. Zhang, Z. Zhai, C. Wang, M. Zhao, Y. Ma, X. Zhang, L. Weng, M. Zhang, Z. Guo, *Macromol. Chem. Phys.* **2017**, *218*, 1700357; b) H. Gu, H. Zhang, C. Ma, X. Xu, Y. Wang, Z. Wang, R. Wei, H. Liu, C. Liu, Q. Shao, X. Mai, Z. Guo, *Carbon* **2019**, *142*, 131; c) Y. He, S. Yang, H. Liu, Q. Shao, Q. Chen, C. Lu, Y. Jiang, C. Liu, Z. Guo, *J. Colloid Interface Sci.* **2018**, *517*, 40; d) B Song, T. Wang, H. Sun, H. Liu, X. Mai, X. Wang, L. Wang, N. Wang, Y. Huang, Z. Guo, *Compos. Sci. Technol.* **2018**, *167*, 515; e) Q. Chen, Q. Yin, A. Dong, Y. Gao, Y. Qian, D. Wang, M. Dong, Q. Shao, H. Liu, B. Han, T. Ding, Z. Guo, N. Wang, *Polymer* **2019**, *169*, 255.

[9] a) M. Zhao, L. Meng, L. Ma, X. Yang, Y. Huang, J. Ryu, A. Shankar, T. Li, C. Yan, Z. Guo, *Compos. Sci. Technol.* **2018**, *154*, 28; b) L. Wang, H. Qiu, C. Liang, P. Song, Y. Han, Y. Han, J. Gu, J. Kong, D. Pan, Z. Guo, *Carbon* **2019**, *141*, 506; c) Y. Zhang, M. Zhao, J. Zhang, Q. Shao, J. Li, H. Li, B. Lin, M. Yu, S. Chen, Z. Guo, *J. Polym. Res.* **2018**, *25*, 130; d) R. Wei, L. Tu, Y. You, C. Zhan, Y. Wang, X. Liu, *Polymer* **2019**, *161*, 162; e) X. Li, S. Zhao, W. Hu, X. Zhang, L. Pei, Z. Wang, *Appl. Surface Sci.* **2019**, in press. https://doi.org/10.1016/j.apsusc.2019.03.114; f) M. Liu, B. Li, B, H. Zhou , C. Chen, Y. Liu, T. Liu, *Chem. Commun.* **2017**, *53*, 2810.

[10] a) Q. Hu, N. Zhou, K. Gong, H. Liu, Q. Liu, D. Sun, Q. Wang, Q. Shao, H. Liu, B. Qiu, Z. Guo, *ACS Sustainable Chem. Eng.* **2019**, *7*, 5912. https://doi.org/10.1021/acssuschemeng.8b05847; b) H. Liu, Q. Li, S. Zhang, R. Yin, X. Liu, Y. He, K. Dai, C. Shan, J. Guo, C. Liu, C. Shen, X. Wang, N. Wang, Z. Wang, R. Wei, Z. Guo, *J. Mater. Chem. C* **2018**, *6*, 12121; c) J. Zhang, H. Li, B. Zhou, Y. Li, K. Dai, G. Zheng, C. Liu, Y. Ma, J. Zhang, N. Wang, C. Shen, Z. Guo, *J. Mater. Chem. C* **2018**, *6*, 8360; d) H. Wei, H. Wang, Y. Xia, D. Cui, Y. Shi, M. Dong, C. Liu, T. Ding, J. Zhang, Y. Ma, N. Wang, Z. Wang, Y. Sun, R. Wei, Z. Guo, *J. Mater. Chem. C* **2018**, *6*, 12446; e) S. Zhang, H. Liu, S. Yang, X. Shi, D. Zhang, C. Shan, L. Mi, C. Liu, C. Shen, Z. Guo, *ACS Appl. Mater. Interfaces* **2019**, *11*, 10922. https://doi.org/10.1021/acsami.9b00900; f) H. Gu, H. Zhang, J. Lin, Q. Shao, D. P. Young, L. Sun, T. D. Shen, Z. Guo, *Polymer* **2018**, *143*, 324.

[11] a) K. Pielichowski, A. Leszczynska, *J. Polym. Eng.* **2005**, *25*, 359; b) T. Liang, L. Qi, Z. Ma, Z. Xiao, Y. Wang, H. Liu, J. Zhang, Z. Guo, C. Liu, W. Xie, T. Ding, N. Lu, *Composites, Part B* **2019**, *166*, 428.

[12] a) K. Pielichowski, A. Leszczynska, *J. Therm. Anal. Calorim.* **2004**, *78*, 631; b) X. Gao, C. Qu, Q. Zhang, Y. Peng, Q. Fu, *Macromol. Mater. Eng.* **2004**, *289*, 41; c) M. Mehrabzadeh, D. Rezaie, *J. Appl. Polym. Sci.* **2002**, *84*, 2573; d) F. Chang, M. Yang, *Polym. Eng. Sci.* **1990**, *30*, 543.

[13] a) M. Dong, Q. Li, H. Liu, C. Liu, E. Wujcik, Q. Shao, T. Ding, X. Mai, C. Shen, Z. Guo, *Polymer* **2018**, *158*, 381; b) J. Li, S. Ge, J. Wang, H. Du, K. Song, Z. Fei, Q. Shao, Z. Guo, *Colloids Surf. A* **2018**, *537*, 334.

[14] M. Dong, C. Wang, H. Liu, C. Liu, C. Shen, J. Zhang, C. Jia, T. Ding, Z. Guo, *Macromol. Mater. Eng.* **2019**. https://doi.org/10.1002/mame.201900010

[15] a) Y. Li, B. Zhou, G. Zheng, X. Liu, T. Li, C. Yan, C. Cheng, K. Dai, C. Liu, C. Shen, Z. Guo, *J. Mater. Chem. C* **2018**, *6*, 2258; b) H. Liu, W. Huang, X. Yang, K. Dai, G. Zheng, C. Liu, C. Shen, X. Yan, J. Guo, Z. Guo, *J. Mater. Chem. C* **2016**, *4*, 4459; c) H. Liu, M. Dong, W. Huang, J. Gao, K. Dai, J. Guo, G. Zheng, C. Liu, C. Shen, Z. Guo, *J. Mater. Chem. C* **2017**, *5*, 73.

[16] X. Gao, C. Qu, Q. Fu, *Polym. Int.* **2004**, *53*, 1666.

[17] J. Santos, J. Guthrie, *J. Chromatogr. A* **2005**, *1070*, 147.

[18] H. Zhang, N. Liu, X. Ran, C. Han, L. Han, Y. Zhuang, L. Dong, *J. Appl. Polym. Sci.* **2012**, *125*, E550.

[19] X. Wang, X. Cui, *Eur. Polym. J.* **2005**, *41*, 871.

[20] G. Kumar, N. Neelakantan, N. Subramanian, *J. Appl. Polym. Sci.* **1994**, *52*, 483.

[21] W. Yang, X. Wang, J. Li, X. Yan, S. Ge, S. Tadakamalla, Z. Guo, *Polym. Eng. Sci.* **2018**, *58*, 1127.

[22] W. Yang, X. Wang, X. Yan, Z. Guo, *Polym. Eng. Sci.* **2017**, *57*, 1119.

[23] Z. Zheng, O. Olayinka, B. Li, *Eng. Sci.* **2018**, *4*, 87.

[24] A. Dong, T. Dai, M. Ren, X. Zhao, S. Zhao, Y. Yuan, Q. Chen, N. Wang, *Eng. Sci.* **2018**. www.doi.org/10.30919/es8d688

[25] G. Yang, C. Xiang, S. Lin, *China Plast. Ind.* **2014**, *42*, 46.

[26] G. Kumar, N. Neelakantan, N. Subramanian, *J. Mater. Sci.* **1995**, *30*, 1480.

[27] Y. Shu, L. Ye, X. Zhao, *Polym.-Plast. Technol. Eng.* **2006**, *45*, 963.

[28] H. Liu, J.Gao, W. Huang , K. Dai, G. Zheng, C. Liu, C. Shen, X. Yan, J. Guo, Z. Guo, *Nanoscale* **2016**, *8*, 12977.

[29] C. Komalan, K. George, P. Kumar, K. Varughese, S. Thomas, *eXPRESS Polym. Lett.* **2007**, *1*, 641.

[30] Y. Pan, D. Schubert, J. Ryu, E. Wujick, C. Liu, C. Shen, X. Liu, *Eng. Sci.* **2018**, *1*, 86.

[31] T. Osswald, *Understanding Polymer Processing*, 2nd ed., Hanser, Munich, Germany **2017**.

[32] J. Mishra, K. Hwang, C. Ha, *Polymer* **2005**, *46*, 1995.

[33] U. Sundararaj, C. Macosko, *Macromolecules* **1995**, *28*, 2647.

[34] a) S. Li, X. Jiang, X. Yang, Y. Bai, L. Shao, *J. Membrane Sci.* **2018**, *570*, 278; b) L. Ma, Y. Zhu, M. Wang, X. Yang, G. Song, Y. Huang, *Compos. Sci. Technol.* **2019**, *170*, 148; c) L. Ma, N. Li, G. Wu, G. Song, X. Li, P. Han, G. Wang, Y. Huang. *Appl. Surf. Sci.* **2018**, *433*, 560; d) X. Li, S. Zhao, W. Hu, X. Zhang, L. Pei, Z. Wang, *Appl. Surf. Sci.* **2019**, *481*, 374; e) H. Zhu, W. Hu, Y. Xu, B. Wang, D. Zheng, Y. Fu, C. Zhang, G. Zhao, Z. Wang, *Appl. Surf. Sci.* **2019**,

463, 427; f) Y. He, Q. Chen, S. Yang, C. Lu, M. Feng, Y. Jiang, G. Cao, J. Zhang, C. Liu, *Composites, Part A* **2018**, *108*, 12; g) H. Gu, X. Xu, M. Dong, P. Xie, Q. Shao, R. Fan, C. Liu, S. Wu, R. Wei, Z. Guo, *Carbon* **2019**, *147*, 550.

[35] X. Jiang, S. Li, S. He, Y. Bai, L. Shao, *J. Mater. Chem. A* **2018**. *6*, 15064.

[36] a) C. Liao, X. Zhu, W. Xie, F. Zeng, S. Yi, H. Cheng, J. Kuang, Y. Deng, T. Cao, *RSC Adv.* **2018**, *8*, 15315; b) P. Xie, B. He, F. Dang, J. Lin, R. Fan, C. Hou, H. Liu, J. Zhang, Y. Ma, Z. Guo, *J. Mater. Chem. C* **2018**, *6*, 8812; c) W. Xie, X. Zhu, J. Kuang, S. Yi, H. Cheng, Z. Guo, Q. He, *J. Magn. Magn. Mater.* **2017**, *432*, 154; d) L. Chen, J. Zhao, L. Wang, F. Peng, H. Liu, J. Zhang, J. Gu, Z. Guo, *Ceramics Inter.* **2019**, in press. https://doi.org/10.1016/j.ceramint.2019.03.052; e) W. Xie, X. Zhu, S. Xu, S. Yi, Z. Guo, J. Kuang, Y. Deng, *RSC Adv.* **2017**, *7*, 32008.

[37] a) H. Gu, H. Zhang, C. Ma, H. Sun, C. Liu, K. Dai, J. Zhang, R. Wei, T. Ding, Z. Guo, *J. Mater. Chem. C* **2019**, *7*, 2353; b) H. Liu, Q. Li, S. Zhang, R. Yin, X. Liu, Y. He, K. Dai, C. Shan, J. Guo, C. Liu, C. Shen, X. Wang, N. Wang, Z. Wang, R. Wei, Z. Guo, *J. Mater. Chem. C* **2018**, *6*, 12121; c) S. Zhang, H. Liu, S. Yang, X. Shi, D. Zhang, C. Shan, L. Mi, C. Liu, C. Shen, Z. Guo, *ACS Appl. Mater. Interfaces* **2019**, *11*, 10922.